JOURNAL OF FORENSIC SCIENCES

J Forensic Sci, March 2011, Vol. 56, No. 2
doi: 10.1111/j.1556-4029.2011.01701.x
Available online at: onlinelibrary.wiley.com

PAPER

ANTHROPOLOGY

Sabrina B. Sholts,[1] *Ph.D.; Phillip L. Walker,*[1,†] *Ph.D.; Susan C. Kuzminsky,*[1] *M.A.; Kevin W.P. Miller,*[2] *Ph.D.; and Sebastian K.T.S. Wärmländer,*[1,3] *Ph.D.*

Identification of Group Affinity from Cross-sectional Contours of the Human Midfacial Skeleton Using Digital Morphometrics and 3D Laser Scanning Technology*,‡

ABSTRACT: Identifying group affinity from human crania is a long-standing problem in forensic and physical anthropology. Many craniofacial differences used in forensic skeletal identification are difficult to quantify, although certain measurements of the midfacial skeleton have shown high predictive value for group classifications. This study presents a new method for analyzing midfacial shape variation between different geographic groups. Three-dimensional laser scan models of 90 crania from three populations were used to obtain cross-sectional midfacial contours defined by three standard craniometric landmarks. Elliptic Fourier transforms of the contours were used to extract Fourier coefficients for statistical analysis. After cross-validation, discriminant functions based on the Fourier coefficients provided an average of 86% correct classifications for crania from the three groups. The high rate of accuracy of this method indicates its usefulness for identifying group affinities among human skeletal remains and demonstrates the advantages of digital 3D model-based analysis in forensic research.

KEYWORDS: forensic science, forensic anthropology, population affinity, cranial morphology, three-dimensional laser scanning, digital morphometrics

Identifying group affinity from human crania is a long-standing problem in forensic and physical anthropology. Group trait differences that are visually distinctive may not be amenable to measurement, and their variation can be difficult to quantify (1). Early anthropologists often recorded these traits in observational terms until systematic cranial measurements were made possible with specialized instruments, such as subtense calipers and simometers (2). As a result, measurements of subtenses, fractions, and linear distances between anatomical landmarks have been used to establish geographic patterns of worldwide craniometric variation. Measurements of facial projection have proven to be particularly useful for differentiating populations (3), and Gill and Hughes (4,5) have devised three indices of midfacial projection that separate European and Native American crania with higher accuracy than discriminant functions based on overall cranial morphology (6). The Gill method has since been tested and refined to optimize its performance in a forensic context, where the assessment of group affinity is a major part of constructing a biological profile for unidentified human remains. However, a drawback of the Gill method is that it does not distinguish groups of different non-European affinity from each other (7,8).

In recent years, technological advances have allowed researchers to quantify craniofacial shape variation using measurements beyond the conventional subtenses and linear distances (9–11), but few methods have found widespread use or broad practical application. As a result, population affinities of unidentified crania are still frequently determined on the basis of traditional craniometric parameters (12,13), even though the inadequacy of those parameters for describing complex shapes and certain craniofacial features has been noted (14).

In this study, a new method for the identification of group affinity based on midfacial skeletal morphology is tested (15). Three-dimensional (3D) digital models of 90 crania representing three different geographic groups were created with a desktop laser scanner. A geometric plane passing through the craniometric landmarks *nasion* and right and left *zygomaxillare* was used to isolate a midfacial region of the cranium and to produce a contour representing several aspects of midfacial curvature. This contour was subjected to elliptic Fourier analysis, and the resulting Fourier coefficients were used to develop discriminant functions that successfully separate the crania according to their affinity group. The high rate of accuracy of this method indicates its potential usefulness for identifying group affinities among unidentified human skeletal remains and demonstrates the advantages of digital 3D model-based analysis in forensic research.

[1]Department of Anthropology, University of California, Santa Barbara, CA 93106-3210.
[2]Forensic Biotechnology Institute of California, California State University, Fresno, 2576 E San Ramon Avenue, M/S ST 104, Fresno, CA 93740.
[3]Division of Biophysics, Arrhenius Laboratories, Stockholm University, 106 91 Stockholm, Sweden.
[†]Posthumous.

*Presented in part at the 18th International Symposium on Human Identification, October 2, 2007, in Los Angeles, CA.
[‡]Supported in part by the National Science Foundation (EAPSI Award 0812894, S.B. Sholts).

Received 24 Aug. 2009; and in revised form 18 Nov. 2009; accepted 28 Nov. 2009.

© 2011 American Academy of Forensic Sciences

Materials

The 90 adult male crania used in this study were recovered by archaeological excavations in Norway, China, and the U.S. Age and sex determinations were made according to the standards for data collection from human skeletal remains (16). The Norwegian crania ($n = 30$) were excavated from the medieval parish graveyards of the St. Hallvard and St. Nicolaus churches in Oslo and are housed at the Anatomical Institute of the University of Oslo, Norway. The Chinese crania ($n = 30$) were excavated from Ming Dynasty tombs in the Yunnan province of southern China and are housed at the Institute of Vertebrate Paleontology and Paleoanthropology in Beijing, China. The (native) Californian crania ($n = 30$) were excavated from several prehistoric cemeteries on Santa Rosa Island off the Southern California coast (site numbers SRI-2, -3, and -41) and are housed at the Santa Barbara Natural History Museum in California, U.S.A.

Methods

3D Model Analysis

Digital models of all crania were created with a NextEngine desktop 3D laser scanner (NextEngine, Inc., Malibu, CA), using a previously described protocol of 16 scans per cranium (17). Scan data were captured at a resolution of 150 dots per inch, and models were rendered with mesh triangles 0.11 cm in size.

Each model was imported into the RapidWorks software version 2.3.4 (Inus Technology, Inc., Malibu, CA; NextEngine, Inc.), where it was repositioned in correct anatomical position within the 3D coordinate system of the software, that is, in alignment with the midsagittal and Frankfurt horizontal plane (18). A midfacial reference plane was then defined using the three standard craniometric landmarks *nasion* and right and left *zygomaxillare* ([14]; Fig. 1*A*). The *y*-axis was redefined along this plane, and the *z*-axis was adjusted for orthogonality. Next, the portion of the model anterior to the midfacial plane was isolated. A plane parallel to the *x*–*z* plane and passing through the lower of the two zygomaxillare landmarks was then created, and the isolated midfacial component of the 3D model was truncated by this second plane to eliminate any morphological differences caused by pre- and postmortem tooth loss. A two-dimensional (2D) outline of the remaining midfacial portion was created using built-in RapidWorks software tools, resulting in a closed contour consisting of *c.* 300 data points (Fig. 1*C*). This procedure was repeated for all 3D cranial models, allowing for comparisons of the midfacial regions of the crania. Before exporting the contour point coordinates in standard *x*–*y* format (*z*-values being constant and thus not used for statistical analysis), the origin of the coordinate system for each model was set at *nasion*, providing a homologous starting point for the subsequent mathematical operations.

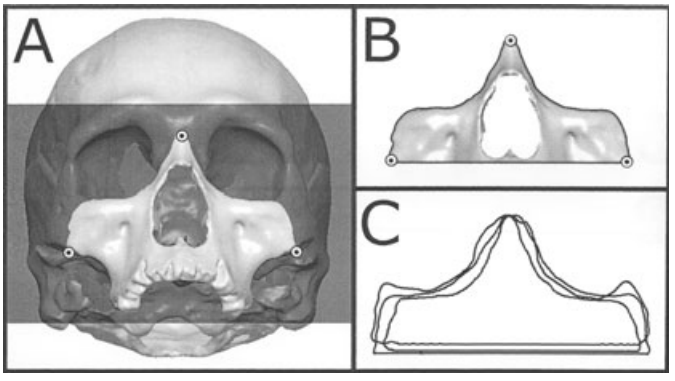

FIG. 1—*The procedure for obtaining midfacial contours from a cranial 3D model. (A) The landmarks nasion and right and left zygomaxillare are identified and used to define a geometric plane, which isolates the anterior midfacial skeleton. (B) A second plane removes the portion below zygomaxillare. (C) The silhouette of the remaining midfacial portion yields the closed contour used for comparisons.*

Elliptic Fourier Transformation

The midfacial *x*- and *y*-contour point coordinates were imported into MATLAB software (The MathWorks, Inc., Natick, MA) as comma-separated values (CSV) (i.e., CSV files), and an Elliptic Fourier transform (19) was employed to convert the contour data into series of Fourier coefficients, using the protocol by Kuhl and Giardina (20). Each closed two-dimensional curve $f(t)$ thus became represented by two traditional Fourier series, one for $x(t)$ and one for $y(t)$:

$$x(t) = A_0 + \sum_{n=1}^{k} a_n \cos(nt) + \sum_{n=1}^{k} b_n \sin(nt) \quad (1)$$

and

$$y(t) = C_0 + \sum_{n=1}^{k} c_n \cos(nt) + \sum_{n=1}^{k} d_n \sin(nt) \quad (2)$$

where n is the harmonic number, k is the maximum harmonic number, and the interval is over 2π (20,21). This expression yields four Fourier coefficients for each harmonic, that is, *x*-sin, *x*-cos, *y*-sin, and *y*-cos, and includes two constants A_0 and C_0 that describe the position of the contour in the arbitrary coordinate system and which should be discarded when comparing Fourier coefficients of the different contours. As the values of the first-order coefficients contain information about the size and orientation of the long and short axes of the contour, these coefficients were used to normalize the sine and cosine series for size and orientation effects. Because each contour contained about 300 points, Fourier coefficients for 64 harmonics could be obtained without violating the specifications of the Nyquist theorem (i.e., $2 \times 64 < 300$; Fig. 2). To reduce the number of coefficients and to discard the phase information which appeared to be less informative for the purpose of this study, the absolute values for the *x*-series, $abs(x_n)$, were calculated from the (a_n, b_n) coefficient pairs:

$$abs(x_n) = \sqrt{a_n^2 + b_n^2} \quad (3)$$

and the corresponding expression was used to obtain the $abs(y_n)$ values from the (c_n, d_n) coefficient pairs. The 64 first absolute values for each of the *x*- and *y*-series were used as independent variables for multivariate statistical analysis (Fig. 3).

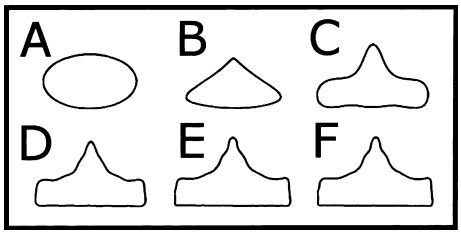

FIG. 2—*Reconstructions of a midfacial contour using different numbers of coefficients* (n)*: (A)* n = *2; (B)* n = *4; (C)* n = *8; (D)* n = *16; (E)* n = *32; and (F)* n = *64.*

Linear Distance Measurements

With each 3D model aligned along the Frankfurt horizontal plane, RapidWorks software tools were used to identify seven craniometric landmarks and measure 13 linear distances between them (Fig. 4). The landmarks used were *nasion* and *zygoorbitale* (left and right) as defined by Howells (14), and *maxillofrontale* (left and right) and *zygomaxillare* (left and right) as defined by Martin and Saller (22). The landmarks and the distances measured between them are shown in Table 1. For each specimen, the geometric mean of the 13 linear distances, d_1–d_{13}, was calculated as $\sqrt[13]{d_1 * d_2 * ... * d_{13}}$. Each measured linear distance was divided by this mean value to achieve size standardization between the measurements from different crania.

Statistical Analysis

The two sets of parameters, that is, the Fourier coefficients and the linear distances, were subjected to two types of statistical analysis. Canonical variate analysis was carried out with SYSTAT 11 software (SYSTAT Software, Inc., Chicago, IL) to compare how well different sets of Fourier coefficients were able to represent the variation between the cranial specimens from the three different populations. Multiple discriminant analysis was carried out using STATA 10 software (StataCorp LP, College Station, TX) to create discriminant functions that were able to classify crania into different affinity groups. Validation of the discriminant functions was accomplished with the leave-one-out technique, where each cranium was independently classified according to discriminant functions based on the other 89 crania in the sample.

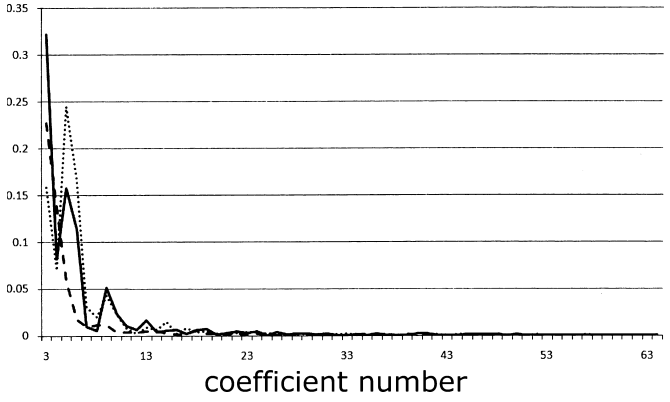

FIG. 3—*Absolute values for the x-series coefficients of one contour from each of the three groups: Norway—dotted line; California—solid line; China—dashed line.*

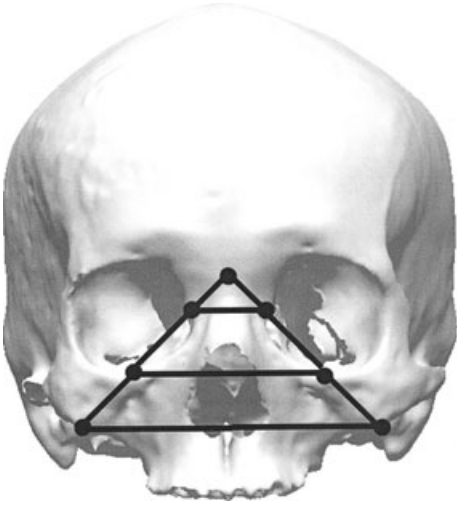

FIG. 4—*For all crania, linear distances were measured between seven landmarks that circumscribe the region of the cranium isolated by the midfacial contour.*

Results

Linear Distance Measurements

For all 3D models, 13 Euclidean linear distances were measured between the seven landmarks presented in Table 1. After standardizing these linear distances for size, they were used to create a set of discriminant functions to classify each of the cranial specimens. The initial performance of these discriminant functions was somewhat successful, yielding correct classifications for 70% of the crania, that is, 23/30 for the Norwegians, 22/30 for the Californians, and 18/30 for the Chinese (Table 2). However, cross-validation of the discriminant functions with the leave-one-out technique resulted in only 57% correct classifications, that is, 16/30 for the Norwegians, 20/30 for the Californians, and 15/30 for the Chinese (Table 2).

Contour Measurements

For all specimens, the midfacial contours passing through *nasion* and right and left *zygomaxillare* were subjected to elliptic Fourier analysis. In Fig. 2, one midfacial contour is reconstructed with inverse Fourier analysis using different number of Fourier coefficients. It is clear that at $n = 64$, the reconstructed contours closely resemble the original ones, with an average deviation of only 0.07 mm. Therefore, the 64 first amplitude coefficients of the respective *x*- and *y*-Fourier series were used as independent variables for statistical analysis. Iterative refinement led to the creation of a set of discriminant functions based on 13 select coefficients, that is, *x*3, *x*10, *x*12, *x*18, *x*20, *x*28, *x*43, *x*41, *x*54, *y*3, *y*27, *y*29, and *y*50. These discriminant functions were able to successfully classify 89% of the crania, with only three to four cases of inaccurate classification per group (Table 3). Cross-validation of the functions using the leave-one-out method showed only a slight decrease in performance, that is, 26/30 for the Norwegians, 25/30 for the Californians, and 26/30 for the Chinese, yielding an average accuracy of 86% (Table 3). A plot of all 90 specimens along the axes of the discriminant functions is shown in Fig. 5.

Discussion

Many recent studies have confirmed the significant effect of population history on the cranial morphology of different groups, even though the evolutionary causes of this variation remain under debate (23–28). Using Howells' (14) worldwide sample, Relethford (29) found the majority of cranial variation to be exhibited within local populations and only a minor part of the total diversity to be displayed between people of different geographic regions—a distribution similar to that found for DNA polymorphisms and genetic markers. Thus, the challenge for craniometric analysis is to identify the traits that distinguish people from different groups or regions.

The results of the present study show that the cross-sectional contour defined by the geometric plane through *nasion* and right and left *zygomaxillare* contains shape information useful for

TABLE 1—*Mean and standard deviation (SD) values in mm for interlandmark distances before size correction, sorted by geographic group.*

		Norway		California		China	
Landmark 1	Landmark 2	Mean	SD	Mean	SD	Mean	SD
Nasion	Zygoorbitale, left	41.7	3.2	43.4	2.5	41.6	2.5
Nasion	Zygoorbitale, right	43.0	3.8	43.9	2.8	42.4	2.8
Nasion	Zygomaxillare, left	72.7	3.3	70.5	4.7	70.4	4.3
Nasion	Zygomaxillare, right	73.7	3.4	70.7	4.6	71.3	4.0
Zygoorbitale, left	Zygoorbitale, right	58.9	4.1	62.5	4.2	58.4	4.4
Zygomaxillare, left	Zygomaxillare, right	94.4	5.8	94.0	6.0	95.6	5.5
Zygoorbitale, left	Zygomaxillare, left	31.7	4.3	28.0	3.5	29.5	3.9
Zygoorbitale, right	Zygomaxillare, right	31.5	3.9	27.7	4.0	29.9	3.9
Nasion	Maxillofrontale, left	15.0	1.6	15.2	2.4	14.2	2.1
Nasion	Maxillofrontale, right	16.2	2.0	15.7	2.0	15.5	1.8
Maxillofrontale, left	Maxillofrontale, right	21.4	2.0	20.6	2.7	20.4	2.6
Maxillofrontale, left	Zygoorbitale, left	28.3	3.3	29.7	2.2	28.5	2.3
Maxillofrontale, right	Zygomaxillare, right	28.7	2.9	29.6	2.8	28.3	2.6

TABLE 2—*Number and percentage of correct classifications by linear discriminant functions based on the 13 interlandmark distance measurements (mean values in bold).*

	Resubstitution		Leave-One-Out	
	No. of Correct	% Correct	No. of Correct	% Correct
Norway (n = 30)	23	77	16	53
California (n = 30)	22	73	20	67
China (n = 30)	18	60	15	50
	21	**70**	**17**	**57**

TABLE 3—*Number and percentage of correct classifications by linear discriminant functions based on the 13 select Fourier coefficients (mean values in bold).*

	Resubstitution		Leave-One-Out	
	No. of Correct	% Correct	No. of Correct	% Correct
Norway (n = 30)	26	87	26	87
California (n = 30)	27	90	25	83
China (n = 30)	27	90	26	87
	27	**89**	**26**	**86**

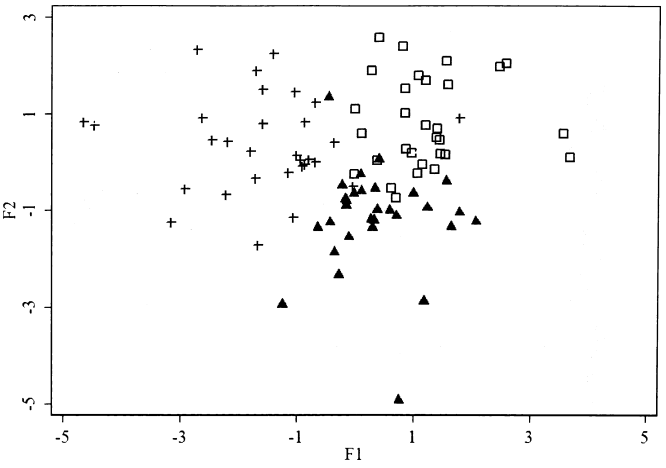

FIG. 5—*The scores of the first (F1) and second (F2) linear discriminant functions based on the 13 select Fourier coefficients, plotted for all crania: Norway—cross; California—square; China—triangle.*

differentiating between Chinese, Norwegian, and Native Californian crania. Using 13 elliptic Fourier coefficients derived from the midfacial contour as variables for statistical analysis, discriminant functions were created, which classify crania from these three groups at an average accuracy rate of 86% with leave-one-out cross-validation (Table 3). This performance is on par with the Gill system, which separates European and non-European crania with an average accuracy rate of 88%, based on six linear distance measurements (three indices) derived from nine landmarks on the midfacial skeleton (4,7,30). However, the discriminant functions based on Fourier coefficients also separate the Native Californians (83% correct classifications) and the Chinese (87% correction classifications) in the sample, which the Gill system is not able to do (Table 3). Although general conclusions cannot be made from the results of this study, given the small size of its sample, the results do suggest that the midfacial contour presented can differentiate European, Asian, and Native American crania on a broader scale. Investigating this possibility with larger sample sizes will be a worthwhile effort, because the results are expected to be important for problems of human identification in places, such as the western U.S. where ancient human remains are often found and turned into Medical Examiners' Offices, and where people of European, Asian, and Native American ancestry have resided concurrently during modern and historic times (31–34).

The relatively poor performance of the discriminant functions based on the 13 linear distances between the seven craniofacial landmarks, which correctly classify only 57% of the sample with the leave-one-out technique (Table 2), illustrates that not all craniofacial measurements contain shape information useful for separating different population groups. Gill and Gilbert (7) describe the European crania in their sample as displaying a relative sharpness of their midfacial features compared with other populations, in the form of a higher and more "pinched" nasal bridge. The six measurements in Gill's system (4) were carefully selected to capture precisely these traits. The lower predictive power of the linear distances measured in this study suggests that they do not adequately quantify these aspects of midfacial variation, despite the fact that they circumscribe the same general region of the skull. The midfacial contour used in this study, on the other hand, appears to be rich in diagnostic shape information. This is not surprising, as the contour traverses multiple bones and combines several features of midfacial morphology, including interorbital breadth, nasal profile depth, and zygomaxillary projection.

Given the ethical and logistical impediments to cross-sectioning a real cranium at the midface, the contour-based approach

demonstrated in this study realistically can only be used with digital 3D models. By the same token, Gill's subtense measurements are difficult to obtain without a simometer (4), although traditional calipers in combination with advanced trigonometry is an alternative method. Hence, both approaches illustrate how new anthropometric methods can be developed by utilizing the unique benefits of novel technology. While digital 3D models can be used to extract the Cartesian coordinate values of landmarks and the linear distances between them, such measurements do not take full advantage of the capacities of 3D technology and they are often more precisely carried out with calipers or 3D digitizers (35–37). The main advantage of 3D imaging is the ability to measure and analyze objects in terms of planes, contours, vectors, and other geometric entities containing shape information. As anthropometric analyses expand to include more computer-based applications for 3D imaging (38), the challenge will be to take advantage of this capacity for geometric operations. Previous research has shown that elliptic Fourier analysis is a promising approach to human skeletal analysis (39–42), and this study presents one application of this method. Because computer programs for 3D model measurements and Fourier analysis are freely available from a range of sources, progress in this field of research is currently limited by the lack of widely accessible databases of 3D models, which would provide samples of appropriate size and diversity to develop and validate new methods of 3D analysis and allow comparisons with forensic specimens.

The type of contour-based analysis demonstrated in this study involves very few subjective decisions, which can be advantageous for evaluations in a medico-legal context. In the process of defining the midfacial contour, the only steps involving subjective decision making are the alignment of the 3D model along the Frankfurt horizontal plane and the location of *nasion* and right and left *zygomaxillare*. For a person with reasonable experience in skeletal biology, these are common procedures that can be performed with high levels of repeatability (43,44). Once the three landmarks have been defined, the midfacial contour can be defined, converted to Fourier coefficients, and analyzed with statistical software without the need for additional measurements or other human manipulations. Conversely, the Gill system involves measurements that are complicated and tools that are somewhat difficult to learn (8).

Conclusions

In this study, the cross-sectional contour defined by the geometric plane through *nasion* and right and left *zygomaxillare* is shown to contain shape information useful for classifying crania by geographic groups. It is also shown that elliptic Fourier analysis is able to convert this shape information into coefficients that are useful for statistical analysis, as discriminant functions based on 13 select Fourier coefficients were able to successfully classify 86% of the 90 crania employed in the study. The successful separation of Norwegian, California Indian, and Chinese crania by this method is an improvement over previous systems for midfacial classification, which cannot accurately distinguish different non-European groups from each other (4,7,8,30). Because the method presented requires only a limited number of subjective measurements, it is well suited for use in a legal context.

Acknowledgments

We thank Dr. C. David L. Thomas (University of Melbourne, School of Dental Science), whose Fourier Shape Descriptor program was used to generate the Fourier coefficients of each midfacial profile. We also thank Professors Liu Wu and Wu Xiujie at the Institute of Vertebrate Paleontology and Paleoanthropology in Beijing, Drs. Ray Corbett and John Johnson at the Santa Barbara Natural History Museum, and Professor Per Holck at the Anatomical Institute at the University of Oslo for help with accessing their collections. Comments by two anonymous reviewers and by Dr. Torstein Sjøvold improved the manuscript and are much appreciated.

References

1. Hinkes MJ. Realities of racial determination in a forensic setting. NAPA Bull 1993;13(1):48–53.
2. Brues AM. The once and future diagnosis of race. In: Gill GW, Rhine S, editors. Skeletal attribution of race. Albuquerque, NM: Maxwell Museum of Anthropology, 1990;1–7.
3. Howells WW. Criteria for the selection of osteometric dimension. Am J Phys Anthropol 1960;30:451–8.
4. Gill GW. A forensic test case for a new method of geographical race determination. In: Rathbun TA, Buikstra JE, editors. Human identification: case studies in forensic anthropology. Springfield, IL: Charles C. Thomas, 1984;47–53.
5. Hughes SS. Differences in nasal projection between American Indian and Caucasoid crania. Wyo Contrib Anthropol Histor Arch 1980;2: 97–113.
6. Giles E, Elliot O. Race identification from cranial measurements. J Forensic Sci 1962;7(2):147–57.
7. Gill GW, Gilbert BM. Race identification from the midfacial skeleton: American Blacks and Whites. In: Gill GW, Rhine S, editors. Skeletal attribution of race. Albuquerque, NM: Maxwell Museum of Anthropology, 1990;47–53.
8. Curran BK. The application of measures of midfacial projection for racial classification. In: Gill GW, Rhine S, editors. Skeletal attribution of race. Albuquerque, NM: Maxwell Museum of Anthropology, 1990;55–7.
9. Richtsmeier JT, DeLeon VB, Lele SR. The promise of geometric morphometrics. Yearbook Phys Anthropol 2002;45:63–91.
10. Slice DE, editor. Modern morphometrics in physical anthropology. New York, NY: Kluwer Academic/Plenum Press, 2005.
11. Zelditch ML, Swiderski DL, Sheets HD, Fink WL. Geometric morphometrics for biologists: a primer. London, UK: Elsevier Academic Press, 2004.
12. Ousley SD, Jantz RL. FORDISC 2.0: Personal computer forensic discriminant functions. Knoxville, TN: University of Tenessee, 1996.
13. Wright R. Detection of likely ancestry using CRANID [online], In: Oxenham M, editor. Forensic approaches to death, disaster and abuse. Bowen Hills, Qld.: Australian Academic Press, 2008;111–22, http://search.informit.com.au/documentSummary;dn=804323190860089;res=IELHEA (accessed January 24, 2011).
14. Howells WW. Cranial variation in man. Cambridge, UK: Harvard University Press, 1973.
15. Sholts S, Miller K, Wärmländer S, Walker PL. The application of three-dimensional midfacial profiling in the identification of human skeletal remains. Proceedings of the 18th International Symposium on Human Identification; 2007 Oct 1–4; Hollywood, CA, http://www.promega.com/geneticidproc/ussymp18proc/abstracts.htm (accessed January 19, 2011).
16. Buikstra JE, Ubelaker DH, editors. Standards for data collection from human skeletal remains. Fayetteville, AK: Arkansas Archaeological Survey, 1994.
17. Sholts SB, Wärmländer SKTS, Flores L, Miller K, Walker PL. Variation in the measurement of cranial volume and surface area using 3D laser scanning technology. J Forensic Sci 2010;55(4):871–6.
18. Garson JG. The Frankfort Craniometric Agreement, with critical remarks thereon. J Anthropol Inst Great Britain Ireland 1885;14:64–83.
19. Thomas CDL. Fourier shape descriptor program, version 2.2.1. Melbourne, Australia: Oral Anatomy, Medicine and Surgery Unit, School of Dental Science, University of Melbourne, 2005.
20. Kuhl FP, Giardina CR. Elliptic Fourier features of a closed contour. Comput Graph Image Processing 1982;18:236–58.
21. Lestrel PE, editor. Fourier descriptors and their applications in biology. Cambridge, UK: Cambridge University Press, 1997.
22. Martin R, Saller K. Lehrbuch der Anthropologie. Stuttgart, Germany: Gustav Fischer Verlag, 1957.

23. Betti L, Balloux F, Amos W, Hanihara T, Manica A. Distance from Africa, not climate, explains within-population phenotypic diversity in humans. Proc R Soc B 2009;276:809–14.
24. Hubbe M, Neves WA. On the misclassification of human crania. Curr Anthropol 2007;48(2):285.
25. Konigsberg LW, Algee-Hewitt BFB. Estimation and evidence in forensic anthropology: sex and race. Am J Phys Anthropol 2009;139:77–90.
26. Ousley S, Jantz RL, Freid D. Understanding race and human variation: why forensic anthropologists are good at identifying race. Am J Phys Anthropol 2009;139:68–76.
27. Roseman CC. Detecting interregionally diversifying natural selection on modern human cranial form by using matched molecular and morphometric data. Proc Natl Acad Sci USA 2004;101(35):12824–9.
28. Weaver TD, Roseman CC, Stringer CB. Close correspondence between quantitative- and molecular-genetic divergence times for Neanderthals and modern humans. Proc Natl Acad Sci USA 2008;105(12):4645–9.
29. Relethford JR. Apportionment of global human genetic diversity based on craniometrics and skin color. Am J Phys Anthropol 2002;118:393–8.
30. Gill GW, Hughes SS, Bennett SM, Gilbert BM. Racial identification from the midfacial skeleton with special reference to American Indians and Whites. J Forensic Sci 1988;33(1):92–9.
31. Bentz L, Schwemmer R. The rise and fall of the Chinese fisheries in California. In: Cassel SL, editor. The Chinese in America: a history from Gold Mountain to the new millenium. Walnut Creek, CA: AltaMira Press, 2002;140–55.
32. Berryman JA. Archival information, abalone shell, broken pots, hearths, and windbreaks: clues to identifying nineteenth-century California abalone collection and processing sites, San Clemente Island: a case study [Doctoral dissertation]. Riverside (CA): University of California, 1995.
33. Braje TJ, Erlandson JM, Rick TC. An historic Chinese abalone fishery on California's Northern Channel Islands. Historical Archaeology 2007;41(4):117–28.
34. Erlandson JM, Bartoy K. Cabrillo, the Chumash, and Old World diseases. J California Great Basin Anthropol 1995;17:153–73.
35. Aung SC, Ngim RCK, Lee ST. Evaluation of the laser scanner as a surface measuring tool and its accuracy compared with direct facial anthropometric instruments. Br J Plast Surg 1995;48:551–8.
36. Richtsmeier JT, Paik CT, Elfert PC, Cole TM, Dahlman HR. Precision, repeatability, and validation of the localization of cranial landmarks using computed tomography scans. Cleft Palate Craniofac J 1995;32: 217–27.
37. Valeri CJ, Cole TM, Lele S, Richtsmeier JT. Capturing data from three-dimensional surfaces using fuzzy landmarks. Am J Phys Anthropol 1998;107(1):113–24.
38. Weber GW, Schaefer K, Prossinger H, Gunz P, Mitterocker P, Seidler H. Virtual anthropology: the digital evolution in anthropological sciences. J Physiol Anthropol Appl Hum Sci 2001;20(2):69–80.
39. Ferrario VF, Sforza C, Guazzi M, Serrao G. Elliptic Fourier analysis of mandibular shape. J Craniofac Genet Dev Biol 1996;16(4):208–17.
40. Daegling DJ, Jungers WL. Elliptical Fourier analysis of symphyseal shape in great ape mandibles. J Human Evol 2000;39(1):107–22.
41. Friess M, Baylac M. Exploring artificial cranial deformation using elliptic Fourier analysis of Procrustes outlines. Am J Phys Anthropol 2003; 122(1):11–22.
42. Lestrel PE, Roche AF. Cranial base shape variation with age: a longitudinal study of shape using Fourier analysis. Hum Biol 1986;58(4):527–40.
43. Ross AH, Williams S. Testing repeatability and error of coordinate landmark data acquired from Crania. J Forensic Sci 2008;53(4):782–5.
44. von Cramon-Taubedel N, Frazier BC, Mirazón Lahr M. The problem of assessing landmark error in geometric morphometrics: theory, methods, and modifications. Am J Phys Anthropol 2007;134(1):24–35.

Additional information and reprint requests:
Sebastian K.T.S. Wärmländer, Ph.D.
Division of Biophysics, Arrhenius Laboratories
Stockholm University
106 91, Stockholm
Sweden
E-mail: seb@dbb.su.se